Article

Techno-Economic and Environmental Analysis of Decommissioned Flowline, Umbilical, and Tubular for Breakwaters

Xihong Zhang [1,*], Wahidul K. Biswas [2], Andy Watt [3], Lendyn Philip [3] and Shaun Sadler [3,4]

1 School of Civil and Mechanical Engineering, Curtin University, 6102 Bentley, Australia
2 Sustainable Engineering Group, Curtin University, 6102 Bentley, Australia
3 Woodside Energy, 6000 Perth, Australia
4 Centre of Decommissioning Australia, 6000 Perth, Australia
* Correspondence: xihong.zhang@curtin.edu.au; Tel.: +61-(8)-9266-5287

Abstract: This paper presents the application of recycled tubular, flowline, and umbilical in coastal protection structures. Flowline and tubular are found to improve the load resistance capacity of concrete beams. Embedment of flowline, umbilical, and tubular into concrete beams would be beneficial to the structural performance, which do not noticeably alter the initial cracking strength of the concrete beam but will provide good post-cracking resistance. A techno-economic analysis was performed, which revealed that coastal protection concrete structures with decommissioned components accounting for more than 25% of the concrete weight could be both economically viable and environmentally friendly options. Since global warming is the most dominant environmental impact (i.e., 63%), recycling these decommissioned components from offshore structures could impose positive environmental impacts. Given the limited supply of construction materials in the remote coastal area as well as its proximity to decommissioned oil and gas rig sites, these decommissioned components could have great potential for use as construction materials in the coastal areas adjacent to the oil exploration. This preliminary study finds no showstopper for the concept of recycling the mentioned decommissioned components as coastal protection concrete structures from structural performance, environmental impact, and economic perspectives.

Keywords: decommissioned components; concrete structures environmental impacts; eco-efficiency; life-cycle assessment

1. Introduction

1.1. Background

Decommissioning of Australian oil and gas infrastructures is an emerging challenge for oil and gas companies, which in the meantime, also provides new potential and opportunities in supporting the circular economy. The large number of decommissioned tubulars, flowlines, and umbilicals from subsea infrastructures could lead to a substantial amount of waste for landfills, potential environmental contaminants, complex logistics, and high transportation costs (according to the data from the Centre of Decommissioning Australia, there are estimated 1700 km flowlines, 1500 km umbilicals, and 126 flexible risers and dynamic umbilicals in Australia to be decommissioned between 2020 and 2030). Successful recycling of these decommissioned components will provide cost benefits to offset the estimated financial liability to remove various forms of production infrastructures. Effective and efficient waste management options are being sought that can accommodate the tubulars, flowlines, and umbilicals to be decommissioned in Australia over the next three decades. This project aims to discover a potential solution for recycling decommissioned tubular, flowline, and umbilical into coastal protection reinforced concrete (RC) structures.

Umbilicals and flexible flowlines are constructed from multiple layers of protective and insulating plastic, metal armour, electrical cables, hydraulic hoses, and metal or plastic tubes at their core. Within governments, society, and across the industry, there are rapidly changing views on what is acceptable. Legislative and regulatory changes are currently being considered, and regulatory intervention is increasing. The mixed materials used in the manufacture of the equipment, along with the construction methods, results in a product that is not readily deconstructed or recycled. Developing safe, environmentally friendly, and cost-effective decommissioning methods is of increasing importance for aging assets and new projects alike.

1.2. Coastal Protection Concrete Structure

Large dimension coastal protection structures are commonly made of concrete in which reinforcements are cast internally to provide shear and flexural resistances. Recycled tubular, flowline, and umbilical could serve as reinforcements in coastal protection structures. The corrosion resistance character of tubular, flowline, and umbilical could contribute to the durability performance of these coastal concrete structures. Because of the covering concrete, potential contamination in the decommissioned components could be effectively mitigated. Moreover, since these structures are designed to protect the shore, the consequence of structural failures of any unit is trivial, which would not lead to future safety and liability issues. Last but not least, precast concrete companies for these coastal protection structures are normally located near ports, which would substantially reduce logistics and transportation costs and difficulties for those decommissioned tubular, flowline, and umbilical.

To implement recycling of tubular, flowline, and umbilical in RC structures for coastal protection, properly study the behaviours of concrete with plastics (external coating of flowline and umbilical), high-strength alloy/steel (internal layer of flowline, and tubular) need to be carried out. This is also important for employing these recycled materials in most civil and building materials working with concrete. When concrete is poured into or around tubular, flowline, and umbilical, debonding or poor connection between concrete and plastics/alloys could strongly deteriorate the assumed structural strength and integrity and consequentially lead to quality issues such as concrete spalling damage. It is ad hoc challenges for the decommissioned tubular, flowline, and umbilical that have been servicing under seawater for decades, with marine growth, material deterioration, etc. All these above-mentioned challenges and potential risks are worth proper investigation in the early stage.

This paper implements this concept of recycling tubular, flowline, and umbilical for coastal protection structures in stages: (1) preliminary numerical modelling of RC structures with available dimensions and properties of flowline, umbilical, and tubular; and (2) life-cycle assessment (LCA) to study the carbon footprint in the designed life of the proposed coastal protection structures with the decommissioned subsea components.

1.3. Environmental and Economic Impacts

There are economic and environmental implications for the replacement of decommissioned oil rig wastes with carbon and energy-intensive virgin materials in concrete. For quantifying the environmental implications of the use of decommissioned oil rig wastes in concrete, the indicators considered by the Building Council of Australia have been considered in this research [1]. It is worth noting that the construction industries are responsible for almost 23% [2] of Australia's annual greenhouse gas (GHG) emissions and approximately 20% of the total energy consumption [3]. The improvement in the environmental performance of concrete by maximizing the use of by-products could result in a reduction in the structural performance of the concrete, which could affect the eco-efficiency performance of concrete mixes (i.e., producing environmentally friendly concretes not entailing excessive cost while maintaining the structural performance). The eco-efficiency framework that has already been used by the authors in a similar project has been used [4,5].

2. Materials and Methods

2.1. Concrete Mixes

The target flowlines and umbilicals are from a decommissioned Australian offshore oilfield project. The specifications of tubular follow those of standard drill pipes. Selected flowline, umbilical, and tubular dimensions are considered for the preliminary analysis, which are most suitable for coastal protection structures.

Numerical modelling is performed using the finite element (FE) method to simulate the flexural bending test of RC beam. The methodology of beam flexural testing follows AS 1012.11 [6]. Table 1 summarises the investigated flowline, umbilical and tubular dimensions, as well as the concrete beam dimensions. The dimensions of the RC beam are varied to accommodate different sizes of decommissioned components. A total of 15 types of RC beams are investigated. All the decommissioned components, except Case Umbilical2, are located at the centre of the beam, as shown in Figure 1. Such a layout is for construction easiness, which will also provide flexural and shear resistance for the concrete structure. In Case M3U2, two pieces of 92 mm diameter umbilicals are cast in concrete to maximize the consumable of the recycling materials. Following AS3600 [7], the exposure classification of A2 is assumed for all beams with sufficient concrete cover against the coastal environment.
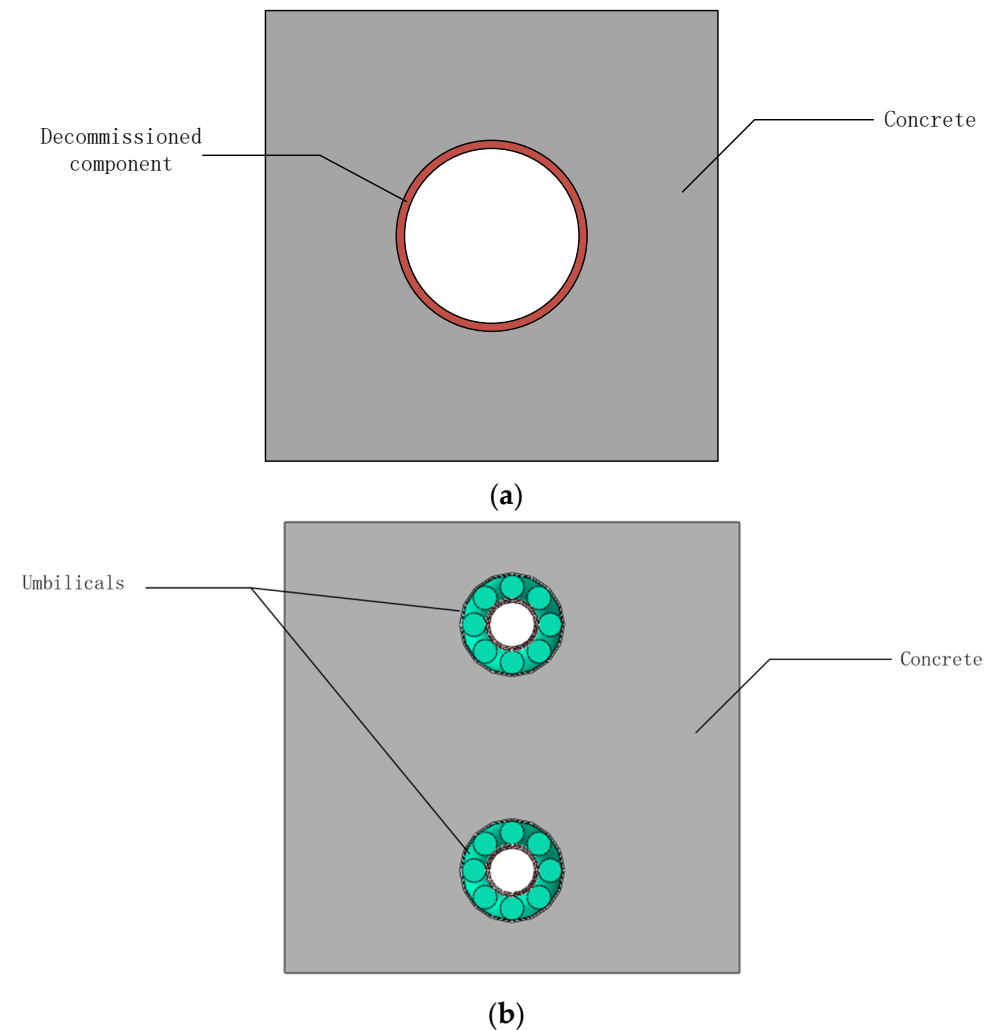

(a)

(b)

Figure 1. Schematic of beam cross-section. (**a**) General cross-section of the beam. (**b**) Cross-section of M3U2.

Table 1. Summary of flowline, umbilical, and tubular dimensions and RC beam dimensions.

Case No.	Span (L) (mm)	Width (B) (mm)	Depth (D) (mm)	Component Type	Component Diameter (d_c) (mm)	d_c/D
R0S1	1600	400	400	N/A	N/A	N/A
R0S2	2080	520	520	N/A	N/A	N/A
R0S3	2400	600	600	N/A	N/A	N/A
M2F1	1600	400	400	flowline	214	0.54
M2F2	2080	520	520	flowline	214	0.41
M2F3	2400	600	600	flowline	336	0.56
M2F4	2400	600	600	flowline	352	0.59
M2F5	2400	600	600	flowline	382	0.64
M1T1	1600	400	400	tubular	140	0.35
M1T2	2080	520	520	tubular	320	0.62
M3U1	1600	400	400	umbilical	92	0.23
M3U2	1600	400	400	umbilical	92 (2 pcs)	0.23
M3U3	1600	400	400	umbilical	167	0.42
M3U4	2400	600	600	umbilical	167	0.28
M3U5	2400	600	600	umbilical	184	0.31

Note: Reference RC beams with plain concrete are considered listed as R0S1, R0S2, and R0S3.

2.2. Material Properties

2.2.1. Concrete

Table 2 lists the concrete strength requirement for Accropodes (one popular coastal protection concrete structure). As the largest beam used in this study has a volume of 0.256 m^3, which is lower than 4 m^3, C25/30 concrete is used to meet the requirement. Concrete class C25/30 in Eurocode 2 [8] corresponds to the concrete class N25 in AS3600: 2018 [7]. Hence, N25 is chosen for all the simulations.

Table 2. Concrete strength specification for Accropode.

	Units $\leq$ 4 m^3	5 m^3 $\leq$ Units $\leq$ 15 m^3	Units > 15 m^3
Concrete class	C25/30	C30/35	C30/35
Tensile strength	2.5 MPa	3.0 MPa	3.0 MPa

The concrete damaged plasticity (CDP) model is employed to simulate the mechanical behaviours of concrete [9], with parameters based on AS3600: 2018 [7]. Mander et al. [10] have verified the accuracy of this material model. The stress–strain curves are shown in Figure 2.
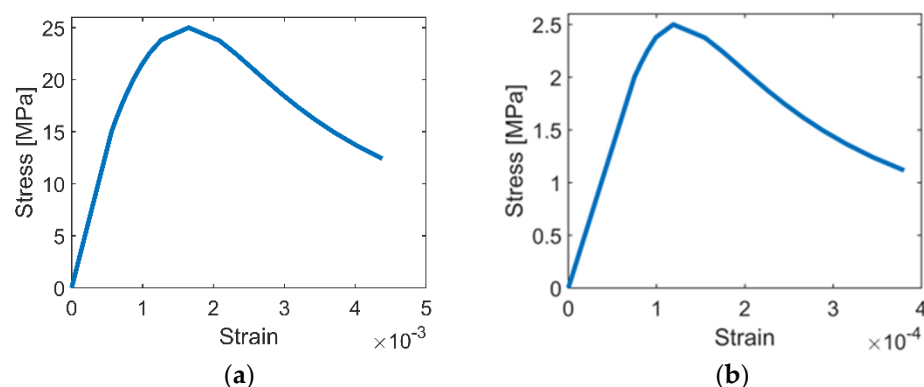
Figure 2. Stress-strain relationship of concrete in concrete damaged plasticity model. (**a**) Compression. (**b**) Tension.

2.2.2. Flowline

Flowlines are modelled following the layout illustrated in Figure 3. Shell elements are employed in the numerical model with layer thicknesses as tabulated in Table 3. Table 3 also summarises the material properties of each layer. The tie constraint is adopted to simulate the bonding between each layer of the flowline. The interaction between the outermost layer (external plastic sheath) and the concrete is most critical, which is modelled using the Coulomb friction model. Hard contact is set for the normal direction, while a friction coefficient of 0.5 is set for the tangential direction. Therefore, potential sliding may occur between the flowline and concrete when the beam is under loading.
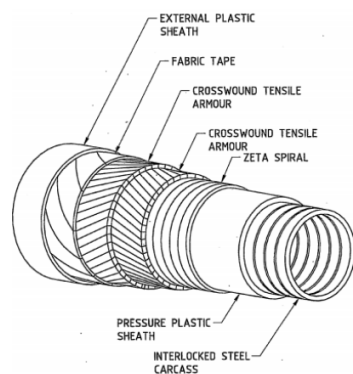

Figure 3. Cross-section of a typical flowline.

Table 3. Thickness and material properties of flowline layers.

Layer	Thickness (mm)	Elastic Modulus (MPa)	Yield Strength (MPa)	Ultimate Strength (MPa)	Ultimate Plastic Strain
External plastic sheath	14.8	2580	63.6	64.5	0.03
Fabric tape	1.15	2100	100	100	0.1
Crosswound armour	2	1480	51	51	0.1
Crosswound armour	3	76,000	1240	1240	0.1
Zeta spiral	10	5.86	8.62	8.62	0.1
Pressure plastic sheath	6.6	3290	49.2	61.8	0.0415
Interlocked steel carcass	10	193,000	290	558	0.1

2.2.3. Umbilical

The cross-sectional layouts of umbilical with different diameters and functionalities could vary substantially, whereas electrical cables, communication wires, water pipes, etc., could exist with different layouts. Nevertheless, some components may not take the load applied to the concrete structures. Therefore, a unified cross-sectional layout is assumed, as shown in Figure 4, to enable the analysis and practical design. This assumption is deemed to be conservative, in which only the plastic sheath and steel armour are considered. A previous study [11] demonstrated the validity of the method. The cross-section comprises three parts, i.e., an inner polypropylene (PP) sheath with a thickness of 3 mm, side wires made of 316 L Austenitic stainless steel with a diameter of 10.5 mm, and an outer PP sheath with a thickness of 2 mm. The steel wires are wrapped around the inner sheath in a helical form, as seen in Figure 5. The material parameters used in the simulation are shown in Table 4. The Coulomb friction model is adopted for the interaction between different layers of the umbilical as well as between the outer sheath of the umbilical and the surrounding concrete. A friction coefficient of 0.5 is assumed.
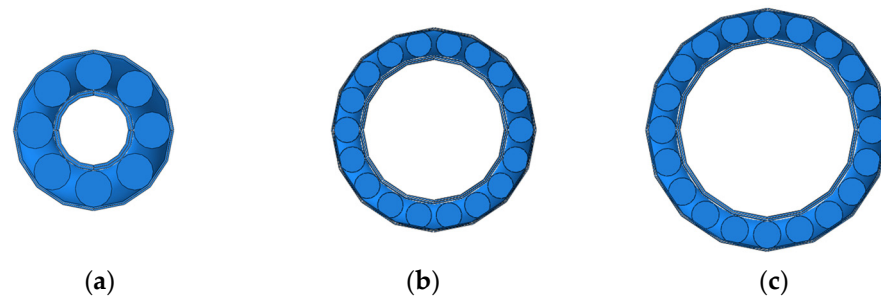
Figure 4. Cross-section of umbilical. (**a**) Diameter = 92 mm. (**b**) Diameter = 167 mm. (**c**) Diameter = 184 mm.
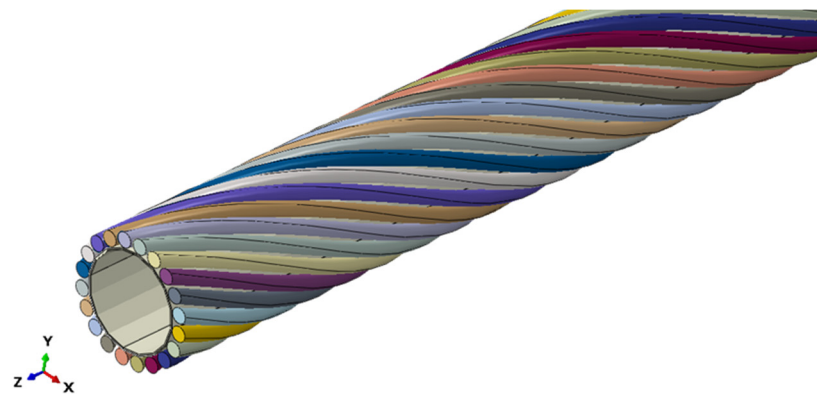

Figure 5. Helical side ropes around inner sheath in umbilical.

Table 4. Material properties of umbilical layers.

Item	Elastic Modulus (MPa)	Yield Strength (MPa)	Ultimate Strength (MPa)	Ultimate Plastic Strain
Outer sheath	1680	33	80	1.312
Side rope	193,000	290	558	0.1
Inner sheath	1680	33	80	1.312

2.2.4. Tubular

Tubulars of two diameters, 140 mm and 320 mm, are considered with a wall thickness of 10 mm in the numerical analyses. Austenitic stainless steel with a volume of 316 L is assumed with the material properties of elastic modulus of 193 GPa, yield strength of 290 MPa, and ultimate strength of 558 MPa.

2.3. Element Type and Mesh Strategy

Considering the complex geometry and layout of the components in the concrete beam, fine-meshed first-order reduced-integration elements are employed for the numerical model. The eight-node first-order reduced-integration solid element is chosen for all solids, including the concrete and the steel material; four-node first-order reduced-integration shell elements S4R are selected for the tubular pipe, all the layers of the flowline and the outer and inner sheaths of the umbilical. A four-node three-dimensional bilinear rigid quadrilateral element is used for the loading rollers and the supporting rollers, which are modelled as rigid.

A mesh convergence study is conducted, which concludes an element size of 25 mm for concrete and 8 mm for the steel bars will yield both accurate enough and computationally efficient performance. For shell elements, each circumference is discretised into 16 elements, as illustrated in Figure 6, to ensure the smaller dimension components are reliably modelled.
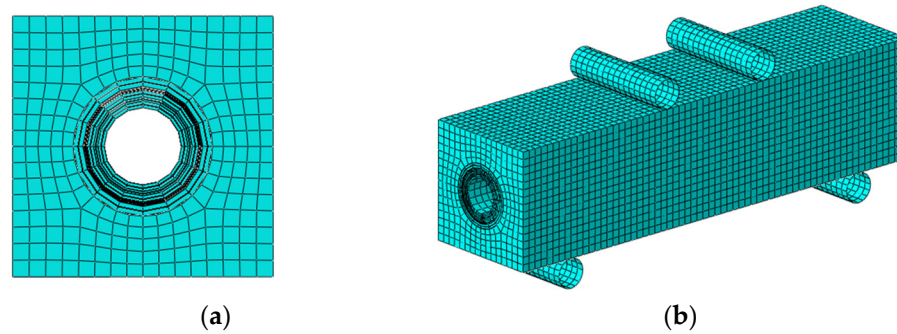
(a) (b)

Figure 6. Example of typical mesh strategy (Case M2F2). (**a**) Cross-section view; (**b**) Overview of model mesh.

2.4. Contact Properties

The contact between the outermost layer of flowline/umbilical and concrete has a hard contact behaviour in the normal direction and a friction coefficient of 0.5 in the tangential direction. Such contact settings are also adopted between the supporting/loading rollers and the RC beam. The contact parameters between the flowline, umbilical and tubular with concrete follow existing studies on the bonding of concrete with plastic and steel [12]. These parameters are subjected to further validation of laboratory testing since the decommissioned components have served in the subsea environment for years with potential surface degradation and marine growth. All these pre-conditions could influence the bonding reinforcement component with concrete. There is no such study yet nor recommended practice.

2.5. Boundary Conditions

The loading is applied to the concrete beam by the loading rollers in a displacement-controlled mode. For the rigid supporting rollers, all degrees of freedom (DOFs) are constrained except the rotational DOF about the axis normal to the loading plane. For the rigid loading rollers, they are allowed to move vertically and rotate about the axis normal to the loading plane, while all the other DOFs are constrained.

2.6. Type of Solver and Solution Process

In light of the complicated contact conditions, explicit analysis is employed in the numerical modelling [13]. Additionally, the element erosion technique is adopted for concrete experiencing large strains, which enables the numerical modelling to simulate the large deformation behaviour of the decommissioned component. The self-weight of the beam is also considered in the analysis. The mass-scaling technique is used to accelerate the computation based on the criterion that the kinetic energy of the model does not exceed 5% of internal energy [9].

2.7. Eco-Efficiency Framework

Eco-efficiency framework is applied to assess the economic, environmental, and eco-efficiency performance of concrete mixes using recycled decommissioned components for coastal protection structures.

The eco-efficiency framework based on Zhang and Biswas [5] is used to compare the eco-efficiency performance of concrete mixes. Firstly, the environmental impacts and costs of concrete mixes are determined to ascertain their eco-efficiency performance. The objective of eco-efficiency is to produce these concrete mixes with reduced environmental impacts and costs. The technological solutions that are used for reducing environmental impacts could increase the costs or vice versa. An eco-efficiency framework is, thus, used to address this dilemma through a comparative assessment process to identify the concrete mixes that deliver better environmental performance in a cost-competitive manner. The

eco-efficiency framework uses both environmental impacts and cost values of concrete mixes to determine their eco-efficiency portfolios for comparison purposes.

The first step of the eco-efficiency assessment (EEA) framework is to carry out a life-cycle assessment to calculate the life-cycle environmental impacts of concrete mixes. The next step calculates the costs of concrete mixes.

2.7.1. Life-Cycle Assessment

The environmental impacts which are relevant to the assessment of Australia's construction sector are determined for each concrete structure design. The impacts listed below are based on the Building Product Innovation Council of Australia [1].

ISO14040-44 guidelines [14] are used to calculate these environmental impacts of the concrete structure design. The steps that this guideline consists of include goal and scope, life-cycle inventory (LCI), life-cycle environmental impact assessment (LCIA), and interpretation. The goal of the LCA is to calculate the environmental impacts due to the use of recycled decommissioned components of oil and gas rigs in concrete structures. This LCA follows a 'cradle to gate' approach, including the raw materials production, transportation of these materials to the point of construction, and the manufacturing of concrete stages. The concrete mix of 1 m^3 is chosen as a functional unit to conduct a mass balance to estimate the amount of energy and materials used during cradle-to-gate stages for developing a life-cycle inventory (LCI).

An LCI needs to be developed prior to the estimation of 14 environmental impacts. The energy consumed in manufacturing these concrete structures with decommissioned flowline, umbilical and tubular is based on Biswas et al. [15]. Table 5 shows the LCIs consisting of inputs, including cement, aggregates, sand, recycled decommissioned components, electricity for manufacturing, and transportation in terms of tonnes per kilometer travelled for 12 concrete structures with reference to the numerical modelling results.

Table 5. Life-cycle inventory of concrete mixtures.

Case No.	Cement	Sand	Aggregate	Decom. Components	Transport	Cutting Energy	Manufacturing
	(kg)	(kg)	(kg)	(kg)	(km)	(Wh)	(Wh)
M1T1	398	553	1261	14	766	266	74.9
M1T2	393	546	1245	41	758	609	74.9
M2F1	373	517	1180	155	723	407	74.9
M2F2	364	506	1153	202	709	407	74.9
M2F3	348	484	1103	291	681	639	74.9
M2F4	311	432	985	498	618	670	74.9
M2F5	296	411	937	580	593	727	74.9
M3U1	397	551	1257	20	764	35.9	74.9
M3U2	393	546	1245	40	758	71.9	74.9
M3U3	397	551	1256	21	764	65.2	74.9
M3U4	395	548	1251	31	761	65.2	74.9
M3U5	373	519	1182	151	724	71.9	74.9
Controlled	401	556	1268	0	770	0.0	74.9

Note: T refers to "Tubular", F refers to "Flowline", U refers to "Umbilical".

The specification of the concrete mixes is based on Eurocode 2 [8], as listed in Table 6.

Table 6. Specification of concrete mixes.

Ingredients	Per m^3	%
Cement	398	18
Sand	566	25
Aggregate	1261	57
Total	2225	100
Water	175	

It is assumed that the decommissioned components will be shipped to Dampier, where they will be cut into designed shapes instead of discarded.

By applying the decommissioned components into the concrete beams, a portion of the original concrete will be saved. The weight of decommissioned components replacing concrete is determined as follows:

- Specific weight of tubular pipes is determined using the information in Rotech Rural [16] and What is piping [17].
- The weights of the flowline and the umbilical are specified from the decommissioned offshore oilfield facilities.
- The thicknesses of the decommissioned components, as shown in Table 3, is an input for determining the cutting energy of three different decommissioned components.
- The cutting energy for tubular is predicted informally by Total Metal Recycling in Western Australia, suggesting that a 400 mm 3-phase cut-off saw would be the best on each diameter. The time for each cut would be about 60 s (+/− 10%). The cut-off saws/cutters would be at about 2000 watts to 2500 watts on a three-phase supply. The specifications of the cutters, as shown in Table 7, are obtained from Wachs [18]. The cutting energy for cutting the decommissioned flowlines was later validated at Curtin University, Australia. A cutting machine (BOMAR, STG440DGH) of 3.7 kW was used to cut a 9 inches flowline in 20 min.

Table 7. Specification of the hydraulic cutter.

Cutter Drive Pneumatic	Worm Gearbox Is Coupled with the Governed Air Motor.
Capacity	4 hp (2.9 kW) hydraulic motor
	1 inch/min of pipe diameter
Work speed	is the cutting speed.
	10 in (254 mm) = 10 min.

Hanson Australia at 455 Beadon Creek Rd, Onslow WA 6710, where the concrete mixes will be produced, will provide the sources of main concrete ingredients (i.e., cement, sand, and aggregates). The distances between concrete ingredients and the concrete manufacturing plant (Table 8) are ascertained using Google earth (Figure 7).

Table 8. Distances between the sources of concrete ingredients and the manufacturing plant.

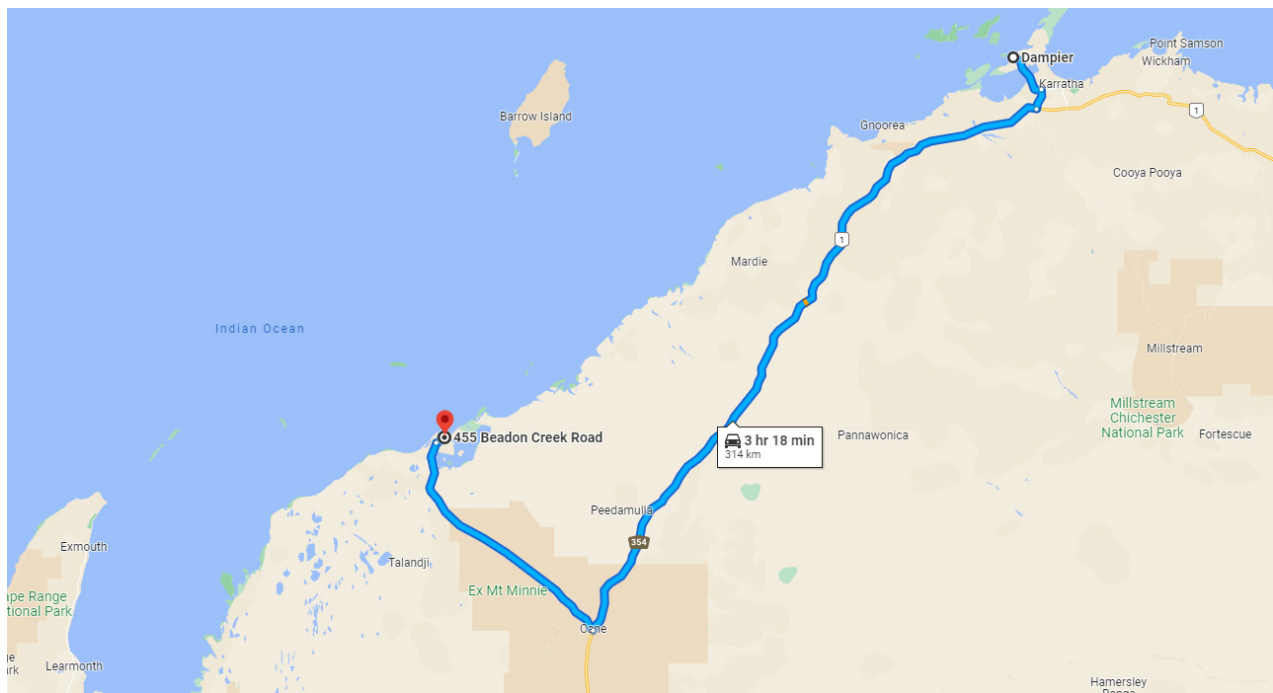| Ingredients	Distance (km)	Locations
Cement	525	Cockburn Cement Port Hedland, 12 Peawah St, Wedgefield WA 6721
Sand	307	Karratha
Aggregate	307	Karratha
Decommission components	314	Dampier port

Figure 7. Northwest Shelf of Western Australia (from Google Earth; the bottom picture shows the distance between the sources of materials and the construction site).

Once the inputs of the LCI of the concrete mixes are entered into SimaPro 9.2 LCA software [19], they are linked to the corresponding emission factor databases. The emission databases of Western Australia were used for most of the inputs to represent the local conditions. These inputs are multiplied by the corresponding emission factors to calculate the 14 environmental impacts of each input (Table 9) [1]. Following this, the environmental impacts of all inputs are added to estimate the total LCIA of each concrete structure design. Australian emission databases are considered for most of the inputs, including electricity, cement, sand, and transportation [20]. New databases had to be developed for gravels and recycled decommissioned components by obtaining the information by directly contacting local industries. A new database for gravels was created in the software by using the information on the amount of fuel consumed in crushing the gravels (i.e., 0.052 megajoules per kg of 10 mm coarse aggregate crushed) [21]. In the case of decommissioned components, the following information and assumptions are considered:

- Emissions from cutting decommissioned components for their use in concrete are considered.
- Natural-gas-fuelled reciprocating engine generating sets that are used in Port Hedland are considered as a supplier of this electricity.
- Emissions from the transportation of decommissioned materials from offshore to Dampier are excluded as they would have been eventually brought back to shore, even though they are not used in the concrete mixes.

Table 9. Impact assessment methods to estimate the environmental impacts [1].

Impact Assessment Method	Environmental Impact	Unit
IPCC GWP 100 [22]	Global warming	t CO_2 eq
Australian indicator set v2.01	Eutrophication Water depletion Land use and ecological diversity	kg PO_4^{3-} eq m^3 H_2O Ha a
ReCiPe 2008 [23]	Human toxicity Terrestrial ecotoxicity Freshwater ecotoxicity Marine ecotoxicity	kg 1,4-DB eq kg 1,4-DB eq kg 1,4-DB eq kg 1,4-DB eq
CML 2 baseline 2001 [24]	Abiotic depletion	kg Sb eq
ReCiPe Midpoint (E) V1.12/Europe Recipe E [25]	Ozone depletion Acidification Photochemical smog Ionising radiation	kg CFC-11 eq kg SO_2 eq kg NMVOC kg U235 eq
TRACI v2.1 [26]	Respiratory inorganics	kg $PM_{2.5}$ eq

Note: eq—equivalent, CO_2—carbon dioxide, PO_4^{3-}—phosphate, Ha. a—hectare years, NMVOC—non-methane volatile organic compounds, U235—uranium 235, Sb—antimony, CFC—cholorofluorocarbon, SO_2—sulphur dioxide, PM—particulate matter.

When the database for crushing was prepared, Australian emission databases for the combustion of diesel for crushing aggregates were used. Hanson concrete uses grid electricity. Australian-first Onslow trial successfully powers the microgrid with 100 percent renewable energy [26]. The emission factor of electricity generated from solar photovoltaic panels is thus considered, as this is the power source for Hanson to manufacture concrete in Onslow.

Not all the environmental impacts can be calculated using the Australian impact method, which is available in the SimaPro LCA software. Since this study had to calculate 14 environmental impacts of this recycled decommission components-based concrete, several relevant methods available in SimaPro 9.2 were calculated following Bengtsson and Howard [1]. The impact assessment methods in Table 9 were used to determine 14 environmental impacts. The input values in the LCI of each rammed earth mix are multiplied by the corresponding emission factors to estimate the environmental impacts.

2.7.2. Economic Costs

The same system boundaries are used in LCA and LCC to produce a consistent, comparable result. The costing is performed based on inputs to produce 1 m^3 of concrete mix. The functional unit is, therefore, the same for both LCA and economic costs to maintain consistency. The same inputs that are available in the life-cycle inventory are used in this cost calculation. Only the labour cost that is not available in the LCI is included in this economic analysis. The market prices are sourced locally to present the local situation. All past prices are converted to 2022 prices using the inflation rate of Australia (Table 10).

Table 10. Cost of inputs of R mixes.

Cement [a]	Sand [b]	Aggregate [b]	Decommissioned Components	Transport [c]	Construction [c]	Labour [c]
(per kg)	(per kg)	(per kg)	(per kWh)	(tkm)	(kWh)	(per hour)
$0.35	$0.04	$0.06	$0.55	$0.09	0.55	32.25

Note: [a] Cockburn Cement Port Hedland, 12 Peawah St, Wedgefield WA 6721. [b] Soil yourself [27]. [c] [5].

2.7.3. Eco-Efficiency Analysis

The economic and environmental impact values of concrete mixes are incorporated into the eco-efficiency analysis (EEA) framework [5] to calculate the eco-efficiency portfolios for comparison purposes.

To provide a link between the environmental impacts and costs, the results are normalised. It is required to normalise the environmental values of concrete mixes with respect to the total environmental impact of a country or a region [28]. Such an approach is considered in this EEA, with the impacts normalised using the Australian gross domestic environmental impacts (GDEI) presented in Table 11.

Table 11. Gross domestic environmental impact and weighting factor of impact indicators used in the LCIA.

Indicator	Units	GDEI	WF (%)
Global Warming Potential	kg CO_2 eq	28,690	19.5
Eutrophication	kg PO_4 eq	19	2.9
Land Use	Ha a	26	20.9
Water Depletion	m^3 H_2O	930	6.2
Terrestrial acidification	kg SO_2 eq	123	3.1
Ozone Depletion	kg CFC^{-11} eq	0.002	3.9
Abiotic Depletion	kg Sb eq	300	8.2
Photochemical Oxidant Formation	kg NMVOC eq	17	2.8
Terrestrial Ecotoxicity	kg 1,4-DB eq	88	10.3
Freshwater Ecotoxicity	kg 1,4-DB eq	172	6.9
Marine Ecotoxicity	kg 1,4-DB eq	12,117,106	7.7
Human Toxicity	kg 1,4-DB eq	3216	2.7
Ionising Radiation	kBq U_{235} eq	1306	1.9
Particulate Matter Formation	kg $PM_{2.5}$ eq	45	3

Normalisation of environmental impact: firstly, the environmental impacts determined in the LCIA are normalised in terms of 'inhabitant equivalents', that is, the equivalent impact per Australian inhabitant per year [28]. The normalised value of each environmental impact of each concrete mix n is calculated using Equation (1):

$$NV_{in} = \frac{LCEI_{in}}{GDEI_{in}} \, [Inh] \tag{1}$$

where

- NV_{in} = the normalised value of the environmental impact *i* of concrete structure *n*;
- $LCEI_{in}$ = the life-cycle environmental impact *i* of concrete structure *n* over all life-cycle stages;
- $GDEI_i$ = the gross domestic environmental impact *i*;
- Inh = the net capita of inhabitants;
- *i* = the *i*th impact category considered in the LCIA.

Prior to aggregating the individual environmental impacts into a single environmental impact value for each concrete mix, the NV_{in} are multiplied by the corresponding weight to reflect the relative degree of importance to the system boundary conditions. The weights of impacts, as shown in Table 11, are used to reflect their importance to Australian conditions [1]. The total environmental impact (EI) for each concrete mix n is determined by weighting and aggregating using Equation (2):

$$EI_n = \sum NV_{in} \times WF_{in} \tag{2}$$

where

- EI_n = the total normalised environmental impact of concrete structure *n*;

- WF_{in} = the weighting factor of impact category i of a concrete mix n;
- The summation of each WF_i must add to 100%.

Normalisation of economic impact: the economic cost is normalised in a similar method by using the Australian Gross Domestic Product in 2021 [29] to reflect the costs in the same units as environmental impacts (i.e., inhabitants per year) [28]. The equation used to calculate the normalised cost is shown in Equation (3):

$$NC_n = \frac{EC_n}{GDP_{cap}} \, [Inh] \tag{3}$$

where

- NC_n = the normalised total cost of concrete structure n;
- EL_n = economic cost of concrete structure n;
- GDP_{cap} = gross domestic product per capita of the region.

2.7.4. Eco-Efficiency Portfolio

To calculate the preliminary portfolio position of each concrete beam design n, Equations (4) and (5) are used:

$$PP_{e,r} = \frac{EI_n}{\left(\frac{EI}{N}\right)} \tag{4}$$

$$PP_{c,r} = \frac{NC_n}{\left(\frac{NC}{N}\right)} \tag{5}$$

where

- $PP_{e,n}$ = environmental impact preliminary portfolio position for option n;
- $PP_{c,n}$ = cost preliminary portfolio position for option n;
- N = refers to the total number of the concrete structures.

In order to describe NC_n, EI_n, and $R_{e,c}$, a visualisation is suggested through the development of the EEA portfolio. An example portfolio is presented in Figure 8, where it can be seen that NC_n is plotted on the abscissa and EI_r on the ordinate [28]. It should be noted that the most eco-efficient options will be located toward the top-right of the portfolio. A diagonal line that runs through the origin is used to decide whether the mix will be eco-efficient. The concrete mix on or above the line is considered eco-efficient. The most eco-efficient option is that which has the largest perpendicular distance above the diagonal line (Figure 8).
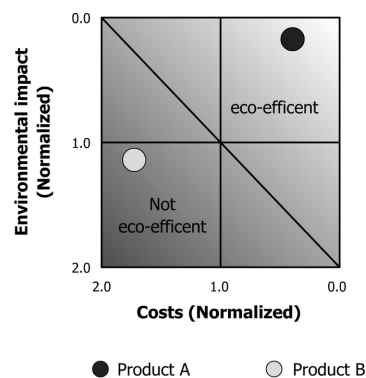

Figure 8. Example eco-efficiency analysis portfolio [30].

Relevance factor: the normalised cost, NC, and normalised environmental impact, EI, form the basis of the EEA portfolio assessment. Therefore, the relevance factor must be calculated to determine whether the NC or EI has a greater influence on the eco-efficiency

performance of the system. This is determined by the ratio of the average environmental impact of all options to the average cost of all options, as shown in Equation (6):

$$R_{e,c} = \frac{\left(\frac{\sum EI_n}{N}\right)}{\left(\frac{\sum NC_n}{N}\right)} \tag{6}$$

where

- $R_{e,c}$ = the relevance factor of environmental impact to cost of all options;
- N = the number of concrete structures to be considered in this portfolio.

To determine the final portfolio position of each option Equations (7) and (8) are used:

$$PP'_{e,n} = \frac{\left[\frac{PP_{e,n}}{N} + \left[PP_{e,n} - \left(\frac{PP_{e,n}}{N}\right)\right] \times \sqrt{R_{e,c}}\right]}{\left[\frac{PP_{e,n}}{N}\right]} \tag{7}$$

$$PP'_{c,n} = \frac{\left[\frac{PP_{c,n}}{N} + \frac{\left[PP_{c,n} - \left(\frac{PP_{c,n}}{N}\right)\right]}{\left[\sqrt{R_{e,c}}\right]}\right]}{\left[\frac{P_n}{N}\right]} \tag{8}$$

where

- $PP'_{e,n}$ = adjusted environmental portfolio position of concrete structure design n;
- $PP'_{c,n}$ = adjusted cost portfolio position of concrete structure design n.

The adjusted portfolio positions are influenced by the relevance factor resulting in a balanced position between the environmental and economic factors [28]. The final positions are plotted graphically to visually assess the potential eco-efficient options. The resulting portfolio is ideal for the comparison of multiple eco-efficient options, a major goal of this research.

3. Results and Discussions

3.1. Flexural Strength

As the dimensions of the beam differ among cases, a nominal flexural stress is defined in Equation (9) to exclude the influence of varying dimensions towards a fair comparison:

$$\sigma_f = \frac{PL}{BD^2} \tag{9}$$

where

- σ_f = nominal flexural stress.

Additionally, the deflection-to-span ratio is defined in Equation (10):

$$d_{rel} = \frac{d}{L}(100\%) \tag{10}$$

where

- d_{rel} = deflection-to-span ratio;
- d = maximum deflection of the beam between the two loading rollers.

Figure 9 shows the nominal flexural stress versus deflection-to-span ratio curves, from which it can be seen that under flexural bending load, the solid concrete beams demonstrate linear elastic response until failure with concrete cracks. Similar initial behaviours are found for the RC beams with flowline, umbilical, and tubular. After initial concrete cracking, the stresses ramp up with further applied displacement when the embedded flowline, umbilical, or tubular comes into effect to provide additional strength to these beams. Much larger secondary peaks compared to the initial peak stress can be found on the stress–

deflection curves for the beams reinforced with flowline or tubular. This demonstrates that flowline and tubular could effectively improve the load-resistance performance of concrete beams. For the umbilicals, the beams exhibit more ductile behaviour, while the resistances of the beams do not appear to improve. This is because the stiffness of the umbilical adopted in the numerical analysis is very low, that concrete crushing would occur under large strain before the umbilical yields. Therefore, optimisation of umbilical locations in the cross-section of the concrete beam should be considered. Table 12 summarises the modelling results, where the performances of the concrete beams with different flowlines, umbilicals, and tubulars are compared with the reference plain concrete beams. The maximum of the nominal flexural stress is defined as the modulus of rupture (flexural strength). It can be seen that the added flowlines could effectively increase the strength of the concrete beams by 40% to 70%. The tubulars can also improve the strength of the concrete beam with considerable enhancement effect, where for Tubular1 (140 mm diameter), the strength of the beam is increased by 117.6%. The concrete beams with added umbilicals (Cases M3U4 and M3U5) show a small strength increase, while for Cases M3U1, M3U2, and M3U3, the strengths of the beams reduced by up to 10%. This is because of the flexible nature of the umbilical, as discussed above.
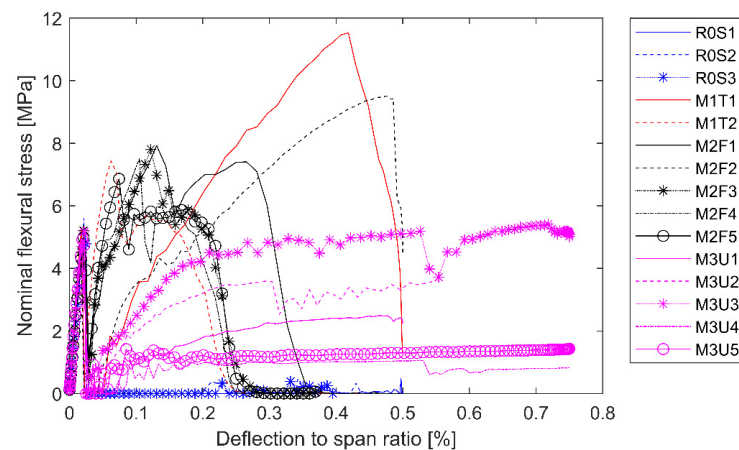

Figure 9. Normalised load–displacement curves.

Table 12. Summary of analysis results.

Case No.	Modulus of Rupture (MPa)	Deflection-to-Span Ratio (%)	Strength Increase
R0S1	5.3	0.02	N/A
R0S2	5.6	0.02	N/A
R0S3	4.79	0.02	N/A
M2F1	7.93	0.13	49.6%
M2F2	9.5	0.48	69.6%
M2F3	7.81	0.12	63.1%
M2F4	7.51	0.1	56.8%
M2F5	6.86	0.07	43.2%
M1T1	11.53	0.42	117.6%
M1T2	7.43	0.06	32.7%
M3U1	4.96	0.02	−6.4%
M3U2	4.75	0.02	−10.4%
M3U3	5.17	0.02	−2.5%
M3U4	4.91	0.02	2.5%
M3U5	4.92	0.02	2.7%

3.2. Damage and Failure Mode

To better understand the response of the concrete beams, the damage contours at initial cracking and ultimate failure states are shown in Figure 10. For the concrete beams with decommissioned components, the failure state is defined as the point when the nominal flexural stress declines to 80% of its peak value. The stiffness degradation (SDEG) scalar is used to depict beam damage, where SDEG = 1 stands for thoroughly damaged material. From Figure 10, it can be found that the initial cracking modes of all the beams are featured with vertical flexural cracks between the two loading rollers, which is resulted from the concrete reaching its tensile strength; cracks quickly extend throughout the reference plain concrete beams leading to the ultimate failure. For the beams with flowlines and tubulars, diagonal cracks can be seen from the loading points to the supports at the ultimate failure states. This illustrates the flexural shear damage of the concrete because the flowlines and the tubulars help to improve the flexural tensile strength of the beams after concrete cracks. For the beams with umbilicals, at ultimate failure states, they fail in a pattern similar to the reference plain concrete beams without forming diagonal shear damage. This shows the umbilicals do not come into effect to pick up the tensile force after concrete tensile cracking.
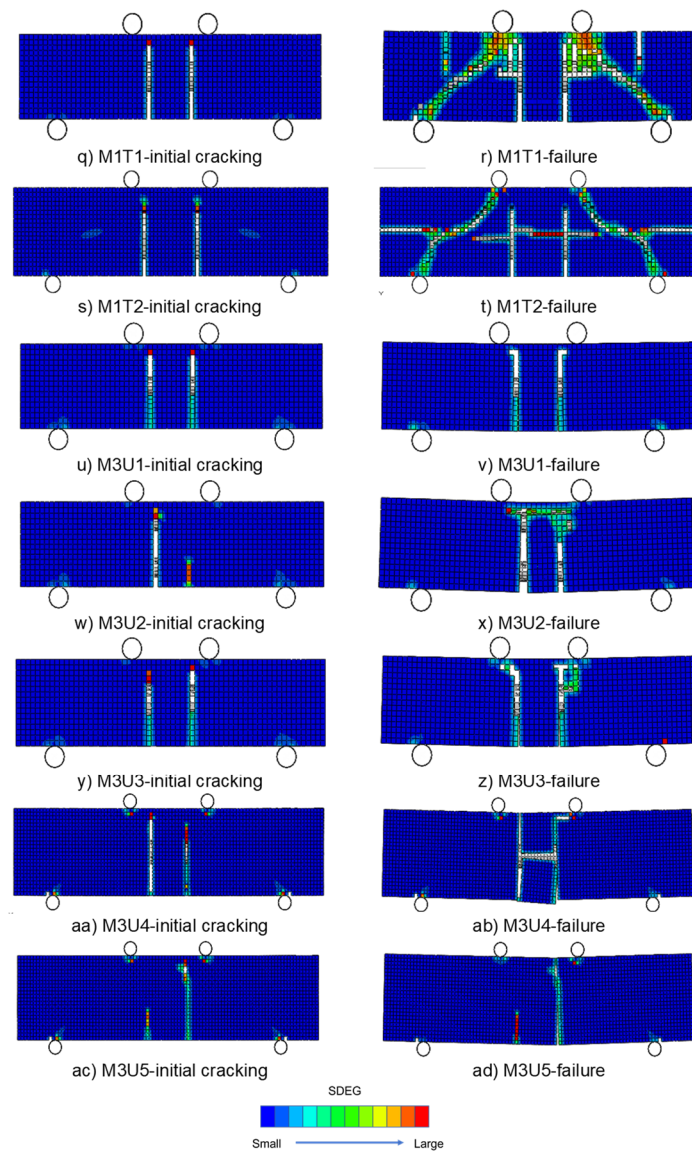

Figure 10. Initial cracking and failure mode of the models.

3.3. Bonding between Outer Surface and Concrete

The bonding between the outer surfaces of the flowline and umbilical with concrete is one of the primary concerns for the application of these decommissioned components into concrete structures. Proper bonding is required for load transfer from concrete to the higher-strength steel layers. In the numerical modelling of this study, the conventional Coulomb friction model with a coefficient of 0.5 is applied. Under gradually increased loading to the concrete beams, sliding is monitored between the outer layer and the concrete. Figure 11 shows the accumulated sliding distance at the instant when initial cracking occurs to concrete. A maximum slippage of 0.3 mm is found between the outer layer of the flowline and concrete in the beam of Case M2F3, while 0.2 mm slippage is found for the beam of Case M3U2. These slippages make the concrete resist the tensile stress from the applied load independently. Thus, similar patterns in flexural cracking are formed in these beams, like the reference plain concrete beams. This is why the addition of flowline and umbilical does not have a noticeable influence on concrete.
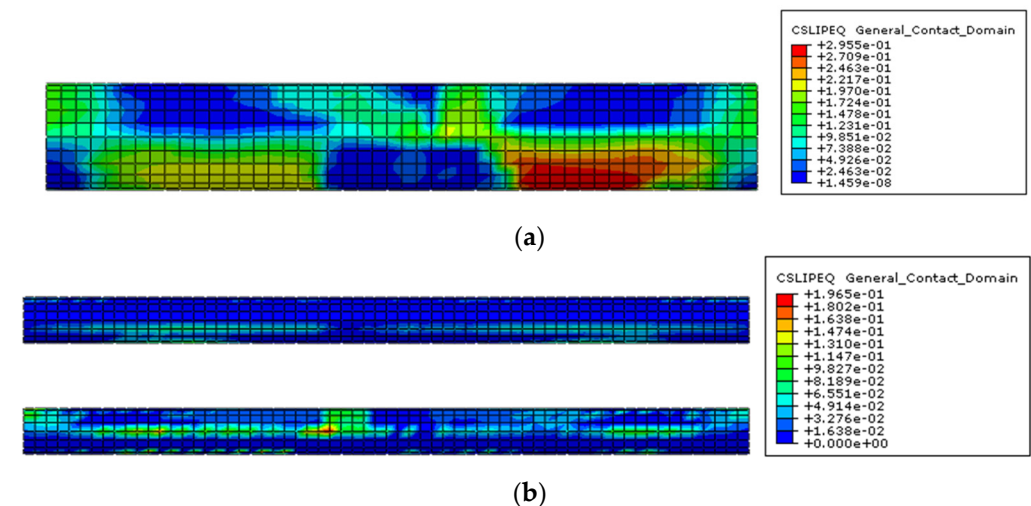

(a)

(b)

Figure 11. Slippage between component surface and concrete at initial cracking (unit: mm). (**a**) M2F3; (**b**) M3U2.

After initial concrete cracking, the deflection of the beam leads to the stretching of the flowline, umbilical, and tubular after the slippage is compensated by the deformation of the beam. These components with very strong steel armour layers come into effect and bear the tensile forces, which results in the concrete beam taking further imposed load. This demonstrates the added components are beneficial to the concrete beam in terms of flexural strength. Bonding between the outer layer and concrete does not appear to be involved in governing the failure of the concrete beam. Because for the practical considering of coastal protection concrete strength whose cross-section height over span length ratio is low. Diagonal shear failure is developed, as illustrated in Figure 10. Thus, bonding between the outer layer and concrete does not play a critical role in the post-cracking phase for the concrete beam. Nevertheless, this finding is based on the assumed friction coefficient between concrete and the outer plastic layer, which is subjected to further laboratory quantitation. Moreover, spalling damage could happen during the service life of coastal protection concrete structures, which needs additional weathering and durability studies.

3.4. Concrete Covering Thickness

Concrete covering thickness shall be considered in the design of RC structures, especially for those exposed to coastal environments against corrosion. This is not critical for the application of decommissioned flowline, umbilical, and tubulars since they are designed with corrosion-resistant materials. Nevertheless, as can be seen in Figure 10, the concrete beam with flowline and tubular added as core eventually fails in diagonal shear

failure mode. This is because the large diameter flowline and tubular reduce the portion of concrete to resist shear forces. By further examining the results summarised in Table 12, the beams of Cases M1T1 and M2F2 have a significantly higher modulus of rupture than others. This is ascribed to their relatively low component diameter to beam height ratios (d_c/D = 0.35 and 0.41, respectively), while the other beams have a d_c/D ratio above 0.5. A low d_c/D value means a thick concrete cover around the component, resulting in a higher capacity against shear loading. A similar phenomenon was mentioned in a previous study [31]. This finding could be beneficial when applying decommissioned flowline, umbilical, and tubular to other concrete structures in civil engineering applications.

3.5. Environmental Impacts

Figure 12 shows the total environmental scores of all concrete structure designs in terms of eco-points. The eco-points for M1C, M1T1, M1T2, M2F1, M2F2, M2F3, M2F4, M2F5, M3U1, M3U2, M3U3, M3U4, and M3U5 are 6.27×10^{-3}, 6.23×10^{-3}, 6.16×10^{-3}, 5.89×10^{-3}, $5.77E \times 10^{-3}$, 5.55×10^{-3}, 5.05×10^{-3}, 4.85×10^{-3}, 6.22×10^{-3}, 6.17×10^{-3}, 6.22×10^{-3}, 6.19×10^{-3}, and 5.90×10^{-3}, respectively. Two concrete structures (i.e., M2F4 and M2F5) meet the eco-efficiency criteria by positioning themselves above the diagonal line. The impact contributing significantly to the overall performance of these mixes is global warming impact, accounting for 63% of the overall environmental impacts of these 13 concrete structure designs. Case M2F5 using the highest amount of recycled decommissioned components (i.e., 36% of the total weight of the concrete mix) has the lowest environmental impacts. The reduction in global warming impact contributes significantly to the overall impact. Figure 13 shows that cement alone accounts for 77% of the total global warming impact. Future studies, therefore, will need to consider the partial replacement of OPC with less carbon-intensive materials having cementitious or pozzolanic properties while maintaining the required level of structural performance. Fly ash, geo-polymer concrete, and ground granular blast furnace slag, which are derived from coal power plants and steel mills, can be considered for partial replacement of cement. In addition, fly ash has been found to be a suitable replacement for OPC in the marine environment for increasing durability [32]. However, about 22% and 26% of the total carbon footprint can be avoided by using M2F4 and M2F5. After the global warming impact, transport accounts for the second largest hotspot (21%) of all concrete structures due to the fact there is no local supplier of concrete ingredients. Cement, sand, aggregate, and the decommissioned components are sourced within radial distances between 300 and 600 km. After GWP, photochemical smog, acidification, and eutrophication are some major environmental impacts resulting mainly from the emissions of dust or particulate matter, NOx, SOx, carbon oxides, and methane from the cement industries. Flowcharts for GWI, eutrophication, photochemical smog, and acidification confirm that cement is the main cause of all these impacts. It should be pointed out that since the transportation of concrete is found to strongly impact the analysis results, optimization of concrete supply should be considered, which could improve environmental impact.

The results of the current LCA in terms of 1 m^3 concrete (i.e., between 348.90 and 515.86 kg CO_2 e-) are comparable to a similar LCA of 1 m^3 of Australian concrete mix (401 kg CO_2 e-) as discussed by Crossin [33] and international studies (361–387 kg CO_2 e-) by Braga et al. [34] and Kurda et al. [35]. Whilst the diversion of this waste from landfills and also the avoidance of the use of land for quarrying associated with the production of virgin gravels result in from this recycling activity, it is not found to be the dominant impact compared to other impacts due to the fact that a large number of atmospheric pollutants are emitted during the supply chain of concrete ingredients. Nevertheless, the environmental impact analysis results could be improved through a port development project where coastal protection structures are deemed to be required as a pre-existing assumption. The application of recycling decommissioned components into coastal protection structures in lieu of landfills.
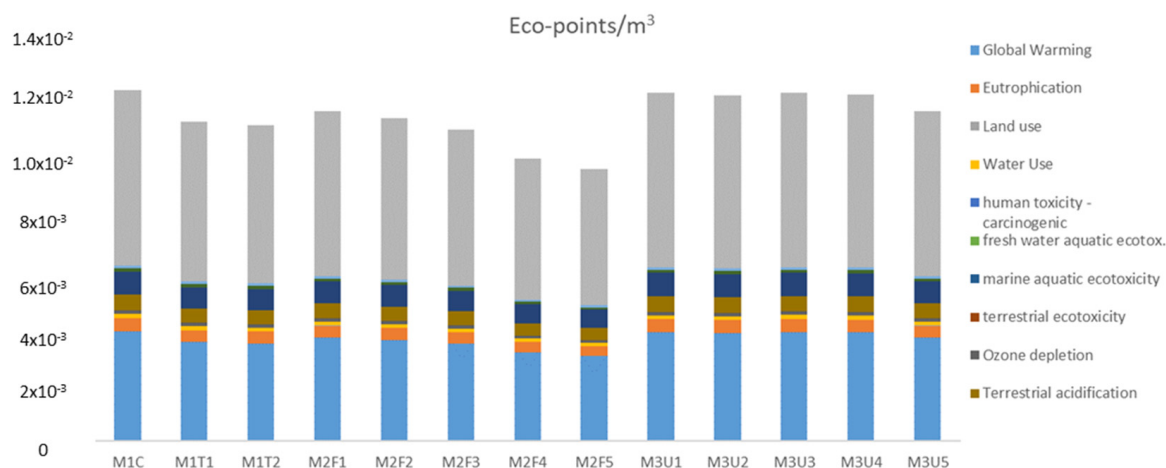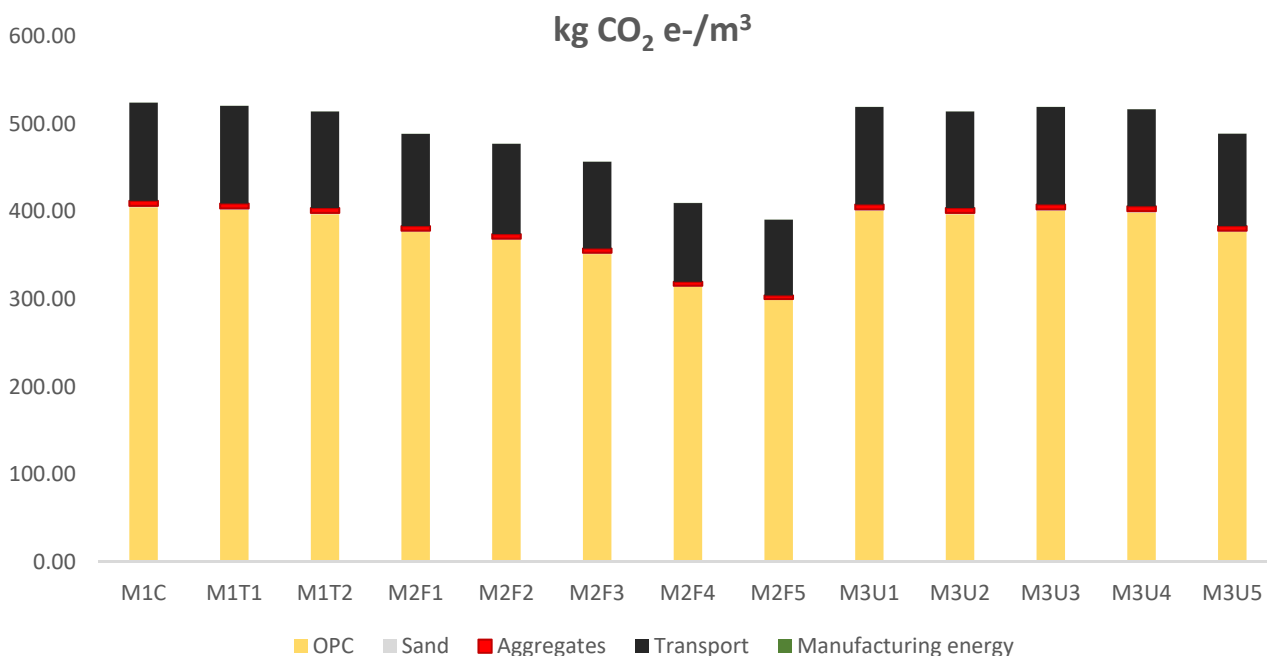
Figure 12. Eco-points of concrete mixes.

Figure 13. Global warming impacts of 13 concrete mixes.

3.6. Economic Costs

The economic costs of concrete mixes vary with the variation of materials of different prices. It appears that the use of the increased amount of decommissioned components would decrease the cost of the proposed concrete structures (Table 13). This is mainly because the costs associated with the use of decommissioned components are very low (between 0.1% and 1%). Only the costs that are associated with the use of decommissioned components are the costs of cutting and its transportation to the construction site. Secondly, its use is replacing expensive concrete materials such as cement and aggregates and the costs associated with transporting them from distant sources. OPC and the transportation of concrete ingredients accounted for 27% and 22% of the total cost, and so the use of decommissioned wastes in concrete as a replacement for these ingredients could significantly reduce the costs of the overall concrete mixes.

Table 13. Summary of costs.

Case	OPC	Sand	Aggregate	Decom. Components	Transport	Construction	Labour	Total
		(per kg)	(per kg)	(per kWh)				
M1C	88.11	20.58	42.28	-	69.33	41.19	31.25	292.74
M1T1	86.50	20.20	41.50	0.95	68.21	41.19	31.25	289.81
M1T2	81.96	19.14	39.32	0.22	65.05	41.19	31.25	278.14
M2F1	81.96	19.14	39.32	0.22	65.05	41.19	31.25	278.14
M2F2	80.11	18.71	38.44	0.22	63.77	41.19	31.25	273.69
M2F3	76.60	17.89	36.75	0.35	61.32	41.19	31.25	265.36
M2F4	68.41	15.98	32.82	0.37	55.62	41.19	31.25	245.64
M2F5	65.12	15.21	31.25	0.40	53.34	41.19	31.25	237.76
M3U1	87.32	20.40	41.89	0.02	68.78	41.19	31.25	290.85
M3U2	86.52	20.21	41.51	0.04	68.23	41.19	31.25	288.95
M3U3	87.29	20.39	41.88	0.04	68.76	41.19	31.25	290.80
M3U4	86.88	20.29	41.68	0.04	68.48	41.19	31.25	289.81
M3U5	82.14	19.19	39.41	0.04	65.18	41.19	31.25	278.40

3.7. Eco-Efficiency Analysis

Three concrete structure designs (M2F3, M2F4, and M2F5) are found eco-efficient due to their lower environmental impact and economic cost values compared to the other designs (Figure 14). Portfolio positions of the concrete structure designs below the diagonal line indicate that these mixes are not eco-efficient. The portfolio positions of 10 concrete structure designs are still below the diagonal line. These concrete structure designs have less than 27% of recycled decommissioned components. For these designs to be eco-efficient, cement needs to be replaced with at least some amount (20–40%) of fly ash, GGBSF, and other cementitious by-products, while maintaining the structural performance. OPC accounts for a significant portion of environmental impacts (63%) and costs (30%), and therefore, the replacement of OPC with less carbon-intensive cementitious materials can reduce impacts and costs at the same time to achieve eco-efficiency.
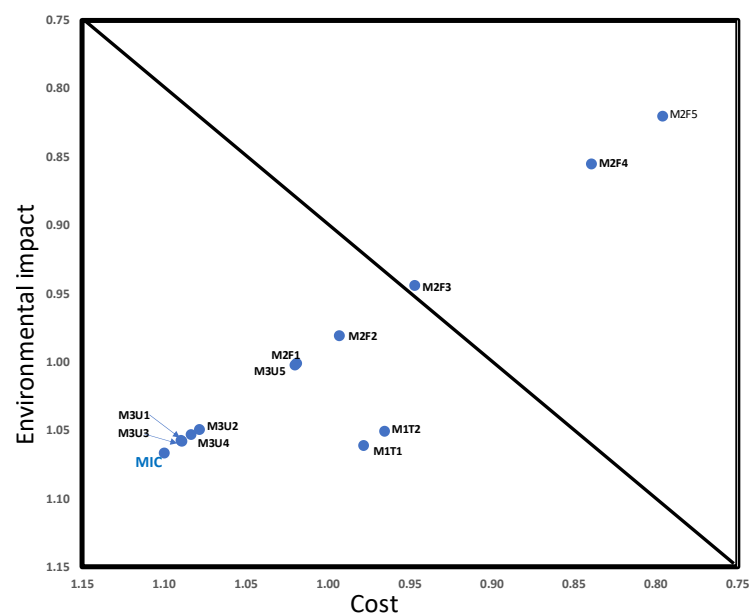

Figure 14. Eco-efficiency portfolio positions of 13 cases.

4. Conclusions

This study performs numerical modelling to preliminarily examine the performance of flowline, umbilical and tubular from decommissioned subsea infrastructures as reinforcement in coastal protection concrete structures. The following conclusions are drawn:

(1) Numerical modelling shows that the embedment of flowline, umbilical, and tubular into concrete beams would be beneficial to the structural performance, which do not noticeably alter the initial cracking strength of the concrete beam but will provide significant post-cracking resistance.

(2) Flexural bending tests find that flowline and tubular will improve the load resistance capacity of concrete beams.

(3) The performance of the umbilical is subjected to further study, which could be improved by optimisation of cross-sectional locations, and/or improved modelling assumptions provided that the bonding properties are quantified.

(4) The accuracy of the preliminary numerical modelling requires further validation, in which bonding between concrete and the outer layer of the flowline and umbilical is important, which will strongly influence the initial cracking behaviour of concrete beams. Further laboratory testing is needed to quantify the bonding behaviour between concrete and the outer layer materials.

(5) Moreover, this study also finds that flowline and tubular could largely increase the flexural bending strength of concrete structures, which will likely lead to a shear-dominated failure mode. Civil engineering applications of adding flowline and tubular in concrete structures should therefore pay special attention to the reduced concrete shear resistance capacity.

(6) Life-cycle analysis reveals that coastal protection concrete structures with decommissioned components accounting for more than 25% of the concrete weight could be both economically viable and environmentally friendly options. Given the limited supply of construction materials in the remote coastal area as well as its proximity to decommissioned oil and gas rig sites, these decommissioned components could have great potential for use as construction materials in concrete mixes.

(7) Global warming is the most dominant impact, accounting for 63% of the total environmental impact. About 22% and 26% of the total carbon footprint can be avoided by using M2F4 and M2F5 concrete mixes, respectively.

(8) Converting decommissioned components to concrete materials and their transportation to the construction site accounts for less than 1% of the total cost of concrete mixes meaning that the maximization of the use of decommissioned components in concrete mixes while maintaining the structural integrity will help achieve the eco-efficiency or a technically, economically, and environmentally viable solution.

Author Contributions: X.Z. was involved in the technical parts, including the literature review, methodology, data curation, formal analysis, investigation, and writing of the structural engineering part of the paper. W.K.B. was involved in the technical parts, including the literature review, methodology, data curation, formal analysis, investigation, and writing of the eco-efficiency part of the paper. A.W. and L.P. provided project management. S.S. was the project sponsor. All authors have read and agreed to the published version of the manuscript.

Data Availability Statement: Not applicable.

Conflicts of Interest: The authors declare no conflict of interest.

References

1. Bengtsson, J.; Howard, N. *A Life Cycle Impact Assessment Method for Use in Australia. Part 1, Classification and Characterization, Report by Edge Environment Pty Ltd. Australia*; Edge Environment Pty Ltd.: Manly, NSW, Australia, 2010.
2. ASBEC. *Capitalising on the Building Sector's Potential to Lessen the Costs of a Broad Based GGHG Emissions Cut*; Centre for International Economics: Canberra, Australia, 2007.
3. Tom Arup, P.H. *Paris UN Climate Conference 2015: Tackling Warming 'Inspires Us'*; Turnbull Tells Summit: Sydney, Australia, 2015.
4. Biswas, W.; Zhang, X. Techno-Assessment of the Use of Recycled Plastic Waste in RE. *Sustainability* **2021**, *13*, 8678. [CrossRef]
5. Zhang, X.; Biswas, W. Development of Eco-efficient bricks—A Life Cycle Assessment Approach. *J. Build. Eng.* **2021**, *42*, 102429. [CrossRef]

6. *AS1012.11:2000*; Methods of Testing Concrete Determination of the Modulus of Rupture. Standards Australia: Sydney, Australia, 2000.

7. Standards Australia. *AS 3600: 2018. Concrete Structures*, 5th ed.; Standards Australia: Sydney, Australia, 2018.

8. European Standards. *Eurocode 2. Design of Concrete Structures*; European Standards: London, UK, 1992.

9. Dassault Systèmes. Abaqus Documentation R2022x. 2022. Available online: http://help.3ds.com/ (accessed on 1 April 2022).

10. Mander, J.B.; Priestley, M.J.; Park, R. Theoretical Stress-Strain Model for Confined Concrete. *J. Struct. Eng.* **1988**, *114*, 1804–1826. [CrossRef]

11. Guttner, W.C.; Santos, C.C.; Pesce, C.P. A finite element method assessment of a Steel Tube Umbilical (STU) cable subjected to crushing load: Comparison between two and three-dimensional approaches. *Marine Struct.* **2017**, *53*, 52–67. [CrossRef]

12. Rabbat, B.G.; Russell, H.G. Friction Coefficient of Steel on Concrete or Grout. *J. Struct. Eng.* **1985**, *111*, 505–515. [CrossRef]

13. Lemos, J. Discrete Element Modeling of the Seismic Behavior of Masonry Construction. *Buildings* **2019**, *9*, 43. [CrossRef]

14. *ISO 14044:2006*; Environmental Management—Life-Cycle Assessment—Requirements and Guidelines. International Organization for Standardization: Geneva, Switzerland, 2006.

15. Biswas, W.K.; Alhorr, Y.; Lawania, K.K.; Sarker, P.K.; Elsarrag, E. Life cycle assessment for environmental product declaration of concrete in the Gulf States. *Sustain. Cities Soc.* **2017**, *35*, 36–46. [CrossRef]

16. Rotech Rural. Steel Pipe Sizes: Dimensions, Diameter & Wall. 2022. Available online: https://rotechrural.com.au/articles/resources/steel-pipe-sizes/ (accessed on 2 May 2022).

17. What Is Piping. Pipe Weight Calculation. 2022. Available online: https://whatispiping.com/pipe-weight-calculation-steel-pipe-weight-chart/ (accessed on 2 May 2022).

18. Wachs, E.H. TRAV-L-CUTTER Pipe Cutter, 600 Knightsbridge Parkway, Lincolnshire, Illinois 60069. 2022. Available online: https://www.ehwachs.com/assets/pdf/35f8af33426a7e42c45ab50926aed48b.pdf (accessed on 2 May 2022).

19. PR'e Consultants. *Simapro Version 8.4*; PR´e Consultants: Amersfoort, The Netherlands, 2021.

20. Life Cycle Strategies Pty Ltd. Australasian Unit Process LCI Library and Methods, Version 2015_02_06. 2015. Available online: http://www.lifecycles.com.au/#!australasian-database/cbm5 (accessed on 5 May 2022).

21. Shaikh, F.A.; Nath, P.; Hosan, A.; John, M.; Biswas, W.K. Sustainability assessment of Recycled Aggregates Concrete mixes Containing Industrial By-Products. *Mater. Today Sustain.* **2019**, *5*, 100013. [CrossRef]

22. IPCC. *Climate Change 2013: The Physical Science Basis. Contribution of Working Group I to the Fifth Assessment Report of the Intergovernmental Panel on Climate Change*; Stocker, T.F., Qin, D., Plattner, G.-K., Tignor, M., Allen, S.K., Boschung, J., Nauels, A., Xia, Y., Bex, V., Midgley, P.M., Eds.; Cambridge University Press: Cambridge, UK; New York, NY, USA, 2013; 1535p.

23. Goedkoop, M.; Oele, M.; Leijting, J.; Ponsioen, T.; Meijer, E. *Introduction to LCA with SimaPro*; PRé Sustainability: Amersfoort, The Netherlands, 2013.

24. Guinee, J. Handbook on life cycle assessment: An operational guide to the ISO standards. *Int. J. Life Cycle Assess.* **2001**, *7*, 311–313. [CrossRef]

25. Bare, J.; Young, D.; Hopton, M. *Tool for the Reduction and Assessment of Chemical and Other Environmental Impacts*; US Environmental Protection Agency: Washington, DC, USA, 2012.

26. Government of Western Australia. Onslow Successfully Powered by 100% Renewable Energy in Trial. 2021. Available online: https://www.mediastatements.wa.gov.au/Pages/McGowan/2021/06/Onslow-successfully-powered-by-100-per-cent-renewable-energy-in-trial.aspx (accessed on 2 May 2022).

27. Soil Yourself. Gravel and Stones. 2022. Available online: https://soilyourself.com.au/gravels-stones/?gclid=EAIaIQobChMIsYTTuYXK9wIVzA5yCh2QdgWCEAAYASAAEgJO_vD_BwE (accessed on 5 May 2022).

28. Kicherer, A.; Schaltegger, S.; Tschochohei, H.; Pozo, B.F. Eco-efficiency. *Int. J. Life Cycle Assess.* **2007**, *12*, 537–543. [CrossRef]

29. Trading Economics. Australia GDP per Capita. 2021. Available online: https://tradingeconomics.com/australia/gdp-per-capita (accessed on 6 May 2022).

30. Arceo, A.; Biswas, W.K.; John, M. Eco-efficiency improvement of Western Australian remote area power supply. *J. Clean. Prod.* **2019**, *230*, 820–834. [CrossRef]

31. Vintzēleou, E.N.; Tassios, T.P. Mathematical models for dowel action under monotonic and cyclic conditions. *Mag. Concr. Res.* **1986**, *38*, 13–22. [CrossRef]

32. Nath, P.; Sarker, P.K.; Biswas, W.K. Effect of fly ash on the service life, carbon footprint and embodied energy of high strength concrete in the marine environment. *Energy Build.* **2018**, *158*, 1694–1702. [CrossRef]

33. Crossin, E. *Comparative Life Cycle Assessment of Concrete Blends*; Centre for Design, RMIT University: Melbourne, Australia, 2012.

34. Braga, A.M.; Silvestre, J.D.; de Brito, J. Compared environmental and economic impact from cradle to gate of concrete with natural and recycled coarse aggregates. *J. Clean. Prod.* **2017**, *162*, 529–543. [CrossRef]

35. Kurda, R.; Silvestre, J.D.; de Brito, J. Life cycle assessment of concrete made with high volume of recycled concrete aggregates and fly ash. *Resour. Conserv. Recycl.* **2018**, *139*, 207–217. [CrossRef]